Modeling in yeast how rDNA introns slow growth and increase desiccation tolerance in lichens

Daniele Armaleo[1] and Lilly Chiou[1]

[1]Department of Biology, Duke University, 27708 Durham, North Carolina

[*]Corresponding author

Abstract

We define a molecular connection between ribosome biogenesis and desiccation tolerance in lichens, widespread symbioses between specialized fungi (mycobionts) and unicellular phototrophs. Our experiments test whether the introns present in the nuclear ribosomal DNA of lichen mycobionts contribute to their anhydrobiosis. Self-splicing introns are found in the rDNA of several eukaryotic microorganisms, but most introns populating lichen rDNA are unable to self-splice, being either degenerate group I introns lacking the sequences needed for catalysis, or spliceosomal introns ectopically present in rDNA. Using CRISPR, we introduced a spliceosomal intron from the rDNA of the lichen fungus *Cladonia grayi* into all nuclear rDNA copies of the yeast *Saccharomyces cerevisiae*, which lacks rDNA introns. Three intron-bearing mutants were constructed with the intron inserted either in the 18S rRNA genes, the 25S rRNA genes, or in both. The mutants removed the introns correctly but had half the rDNA genes of the wildtype strain, grew 4.4 to 6 times slower, and were 40 to 1700 times more desiccation tolerant depending on intron position and number. Intracellular trehalose, a disaccharide implicated in desiccation tolerance, was detected but not at levels compatible with the observed resistance. Extrapolating from yeast to lichen mycobionts we propose that the unique requirement for a splicing machinery by lichen rDNA introns slows down intron splicing and ribosomal assembly. This effect, and the distinctive roles played by group I *vs.* spliceosomal rDNA introns, lead the environmental stress responses of lichen fungi to generate the twin lichen phenotypes of slow growth and desiccation tolerance.

Keywords

Desiccation tolerance, lichens, mycobionts, *Saccharomyces cerevisiae*, rRNA, group I introns, spliceosomal introns, trehalose, CRISPR

Introduction

Desiccation tolerance mechanisms, due to their critical importance for the sustainability of life, have been studied for a long time (LEPRINCE AND BUITINK 2015). More recently, special attention has been devoted to anhydrobiotes, organisms that can survive losing more than 99% of their water (LEPRINCE AND BUITINK 2015; KOSHLAND AND TAPIA 2019). We focus here on ribosome biogenesis as a key node in the control of desiccation tolerance in lichens, stable anhydrobiotic symbioses between specialized fungi (mycobionts) and unicellular green algae or cyanobacteria (photobionts). Assembly and function of ribosomes, which can comprise around 50% of the cell's protein mass, are not only central to translation, but to protein homeostasis as a whole, including proper folding (PECHMANN *et al.* 2013). Protein misfolding and aggregation affect a broad range of phenomena, from human disease (PECHMANN *et al.* 2013) to desiccation tolerance (WELCH *et al.* 2013; KOSHLAND AND TAPIA 2019). Transcriptomic analyses specifically addressing lichen desiccation tolerance suggest ribosomal involvement (JUNTTILA *et al.* 2013; WANG *et al.* 2015). Several ribosomal assembly and translation functions appear to be under purifying selection in the lichen *Cladonia grayi* (ARMALEO *et al.* 2019) suggesting that they play pivotal roles in the anhydrobiotic lichen symbiosis. In yeast, ribosomal network regulation is central to the Environmental Stress Response (ESR) (GASCH *et al.* 2000) and mutations hindering ribosomal assembly enhance desiccation resistance (WELCH *et al.* 2013). Using yeast, we test whether the introns commonly populating the ribosomal DNA of lichen fungi constrain ribosome biogenesis to generate two characteristics typical of lichens: slow growth and extreme desiccation tolerance.

Lichens are ubiquitous in most terrestrial environments, from arid deserts to arctic tundra, forests and mountains. About 20,000 species of mostly Ascomycetes representing 20% of all known fungi are lichen-forming, and associate with about 150 species of lichen-forming algae (SAINI *et al.* 2019). The symbiotic interactions are multifaceted (ARMALEO *et al.* 2019) and center around the carbon fixed by the photobiont and transferred to the mycobiont. The primary mycobionts and photobionts that determine size, shape, color and structure in lichen thalli are accompanied by a varied microbiome of prokaryotes (ASCHENBRENNER *et al.* 2016) and fungi (ARNOLD *et al.* 2009; TUOVINEN *et al.* 2019). Lichen anatomy is complex for microorganisms (HONEGGER 2012) but lacks the water management systems found in plants, such as roots, vascular tissues or waxy cuticles. Lichens employ water-storing polysaccharides and evaporation barriers like cortices, hydrophobins, and secondary compounds to slow down water loss but eventually, within minutes or hours of drying depending on conditions, residual metabolism and transcription come to a complete halt throughout their thalli (JUNTTILA *et al.* 2013; WANG *et al.* 2015; CANDOTTO CARNIEL *et al.* 2020). Yet lichen fungi survive not only extreme water loss, but also exposure to heat, cold and solar radiation. This is in contrast with non-lichenized fungi, which spend most of their life cycles protected within their substrates and survive desiccation through spores. This work focuses exclusively on mycobionts. For a review of lichen desiccation tolerance which includes photobionts, see GASULLA *et al.* (2021).

In fungi, slow growth and stress resistance can be concurrent phenotypes (GASCH 2007), and our analysis centers on how the slow growth of lichens may be linked to their extreme desiccation tolerance. The slow growth of lichens, between 10^{-1} and a few mm/year with outliers in both directions (SANCHO *et al.* 2007), reflects the slow growth of mycobionts, with occasionally measured doubling times of several days in fresh culture (AHMADJIAN 1961; CULBERSON AND ARMALEO 1992). Like other anhydrobiotes, lichens can lose more than 95% of their water content and remain dehydrated for long periods of time, a stress that would kill most organisms (KRANNER

et al. 2008). Frequent desiccation and rehydration induce protein denaturation and aggregation as well as the formation of reactive oxygen species (ROS) that can cause direct damage to DNA, proteins, and lipids. Antioxidants and ROS-processing enzymes, common defenses against stress, are thought to protect also lichens from desiccation damage (KRANNER *et al.* 2008). However, the ability of lichens to repeatedly withstand extreme desiccation suggests the involvement of additional defense mechanisms. Thus, we hypothesized (ARMALEO *et al.* 2019) that the many rDNA introns present in lichen fungi (DEPRIEST 1993b; GARGAS *et al.* 1995; BHATTACHARYA *et al.* 2000; BHATTACHARYA *et al.* 2002) may provide such an extra defense.

The introns relevant to this work are spliceosomal introns and group I introns. Spliceosomal introns, universal among eukaryotes, are normally associated with Polymerase II transcription of protein-coding genes, require specialized host factors to be excised, and perform important regulatory roles (POVERENNAYA AND ROYTBERG 2020). Group I introns are found mostly in ribosomal DNA, and normally form ribozymes able to fold into a conserved structure that catalyzes self-splicing from the transcript without the aid of host factors *in vitro* (CECH 1990), although self-splicing can be aided by maturase proteins facilitating proper folding of the RNA *in vivo* and *in vitro* (LAMBOWITZ *et al.* 1999). Unlike the ubiquitous spliceosomal introns, group I introns occur only across some eukaryotic microorganisms like ciliates, algae, and fungi, and are particularly abundant in plasmodial slime molds (HEDBERG AND JOHANSEN 2013). Experiments with the self-splicing group I intron from the ciliate *Tetrahymena thermophila* in its original host or transferred into yeast rDNA have shown that the intron splices itself co-transcriptionally within seconds (BREHM AND CECH 1983), and that 99% of the introns are removed before the end of 35S pre-rRNA transcription (JACKSON *et al.* 2006), which takes ~2 minutes per molecule (OSHEIM *et al.* 2004) in yeast. Intron presence has no discernible consequences on growth rate (LIN AND VOGT 1998) or other phenotypes (NIELSEN AND ENGBERG 1985). This is why group I introns are commonly considered harmless genetic parasites, including the relatively few group I introns found in the rDNA of non-lichen fungi (HAUGEN *et al.* 2004b; HEDBERG AND JOHANSEN 2013).

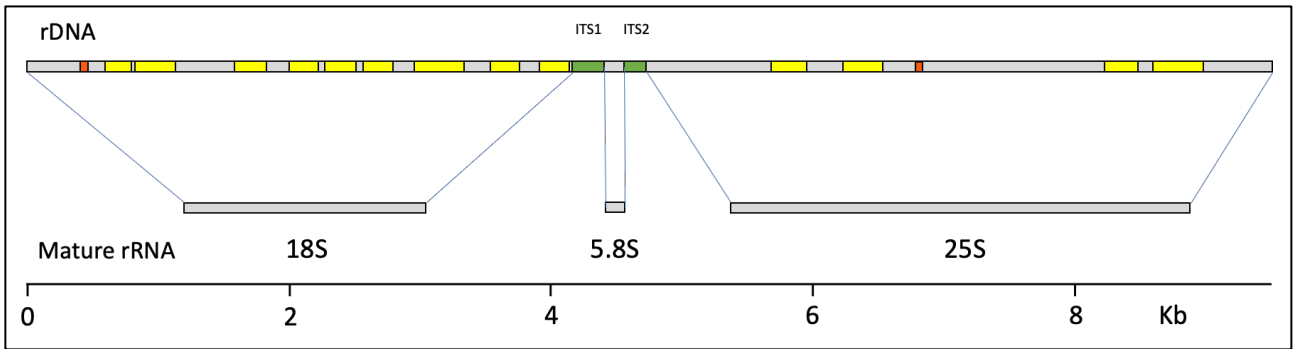

Figure 1. Introns in the rDNA of a single-spore isolate from the lichen fungus *Cladonia grayi* (ARMALEO et al. 2019). Top: the 18S, 5.8S, and 25S region of one rDNA repeat; gray, rRNA coding sequences; green, internal transcribed spacers; yellow, group I introns; orange, spliceosomal introns. Middle: the three mature rRNAs produced from this region. Bottom: scale in kilobases. Sequences were retrieved from https://mycocosm.jgi.doe.gov/Clagr3/Clagr3.info.html

Compared to non-lichen fungi, the rDNA of lichen mycobionts contains many group I introns (Fig.1) and a few ectopic spliceosomal introns (BHATTACHARYA *et al.* 2000) which normally operate only in mRNA. Lichen group I introns tested *in vitro* were found to be "degenerate", i.e. unable to self-splice (DEPRIEST AND BEEN 1992; HAUGEN *et al.* 2004b). This lack of self-splicing has remained a puzzling observation which we reframe here as a universal feature of lichen rDNA introns and a fundamental key to extrapolate our yeast results to lichens. To this end,

Fig. 2 combines self-splicing data across several lichen and non-lichen fungi with their group I intron lengths and includes also group I introns lengths from other microbial eukaryotes. Lichen group I introns, in which all self-splicing tests were negative, are the shortest and lack an average of 100 nucleotides relative to group I introns from non-lichen fungi. The lost sequences have been shown to be necessary for catalysis (HAUGEN *et al.* 2004b). Since such degenerate introns are completely removed from mature rRNA (Fig. 1), a specific group I intron splicing machinery must have evolved in lichens. We place the inability to self-splice and its effects on ribosome biogenesis at the root of the twin lichen phenotypes of slow growth and desiccation resistance. Lack of self-splicing is a characteristic shared in lichens by group I and spliceosomal rDNA introns. There are occasional self-splicing group I introns in lichen fungi, some with endonuclease-encoding sequences (HAUGEN *et al.* 2004a; REEB *et al.* 2007), which would quickly splice themselves out of any significant interference with rRNA processing. Those rare cases do not negate that loss of self-splicing is a prevalent feature of lichen rDNA introns.

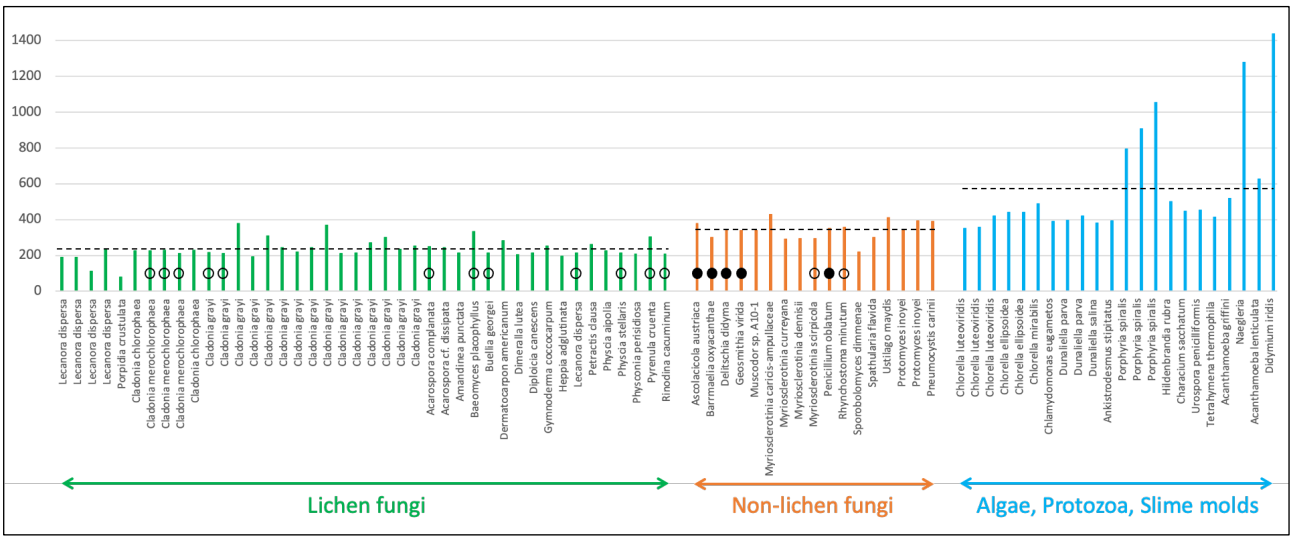

Figure 2. Length and splicing comparisons between group I introns from lichen and non-lichen fungi. Each colored vertical bar represents the length of an intron (nucleotide number on the ordinate). Dotted lines represent the average intron lengths within each of the three groupings (233, 339, and 586 nucleotides respectively). Introns tested for self-splicing *in vitro* by DEPRIEST AND BEEN (1992) and HAUGEN *et al.* (2004b) are highlighted with open circles (no splicing) or filled circles (splicing). Length data were compiled from GARGAS *et al.* (1995), HAUGEN *et al.* (2004b), ARMALEO *et al.* (2019). This is not a comprehensive compilation of all available group I intron data.

To test whether lichen rDNA introns are adaptive against desiccation damage, we used CRISPR to transfer a spliceosomal rDNA intron (the first one on the left in Fig.1) from the lichen *Cladonia grayi* into all 150 rDNA repeats of *S. cerevisiae* (CHIOU AND ARMALEO 2018), which lacks rDNA introns. We inserted the intron at two yeast rDNA sites occupied by introns in *C. grayi*. Three intron-bearing mutants were constructed, with the intron stably inserted either in all copies of the 18S rRNA gene, of the 25S rRNA gene, or of both. Among wildtype and mutant strains, we compared ribosomal DNA repeat number, growth rates, desiccation tolerance, cell morphology and intracellular concentration of trehalose, a disaccharide associated with desiccation resistance in yeast and other organisms (KOSHLAND AND TAPIA 2019). The main effects of the introduced introns were dramatic decreases in growth rate and equally significant increases in desiccation resistance. Based on these and other yeast responses to the introduced introns, we propose a model for how rDNA introns contribute to the anhydrobiotic lifestyle of lichens.

Materials and Methods

Plasmids, strains, and media

DH5α *E. coli* cells containing the plasmid pCAS were obtained from Addgene (#60847). Plasmid pCAS (8.7 Kb) is a kanamycin/G418 shuttle vector carrying the gene for Cas9 and a generic guide RNA expression cassette (RYAN AND CATE 2014). Competent *E. coli* strain DH10B (New England Biolabs, C3019I) was used for transformations. *E. coli* was grown in LB medium (PROTOCOLS 2006) at 37ºC. For *E. coli* transformant selection, kanamycin (ThermoFisher Scientific) was added to the LB medium to 100 mg/L. The yeast strain used was *S. cerevisiae* YJ0 (*MAT**a**, gal4*Δ, *gal80*Δ, *ura3–52, leu2–3, 112 his3, trp1, ade2–101*) (STAFFORD AND MORSE 1998), and was typically grown in YEPD medium (PROTOCOLS 2010) at 30ºC. To select for yeast containing the transforming plasmid, G418 (VWR) was added to the plate medium to 200 mg/L.

Guide sequence introduction into pCAS by inverse PCR, screening, plasmid isolation

The procedure recommended by RYAN *et al.* (2016) to introduce a desired guide sequence into pCAS involves PCR with two self-complementary "guide RNA" primers, followed by DpnI restriction to eliminate the original methylated plasmid before transformation. Since in our hands the yields were very low, we decided instead to update the "inverse PCR" procedure developed for plasmid mutagenesis by HEMSLEY *et al.* (1989). We found that by using two primers which are not

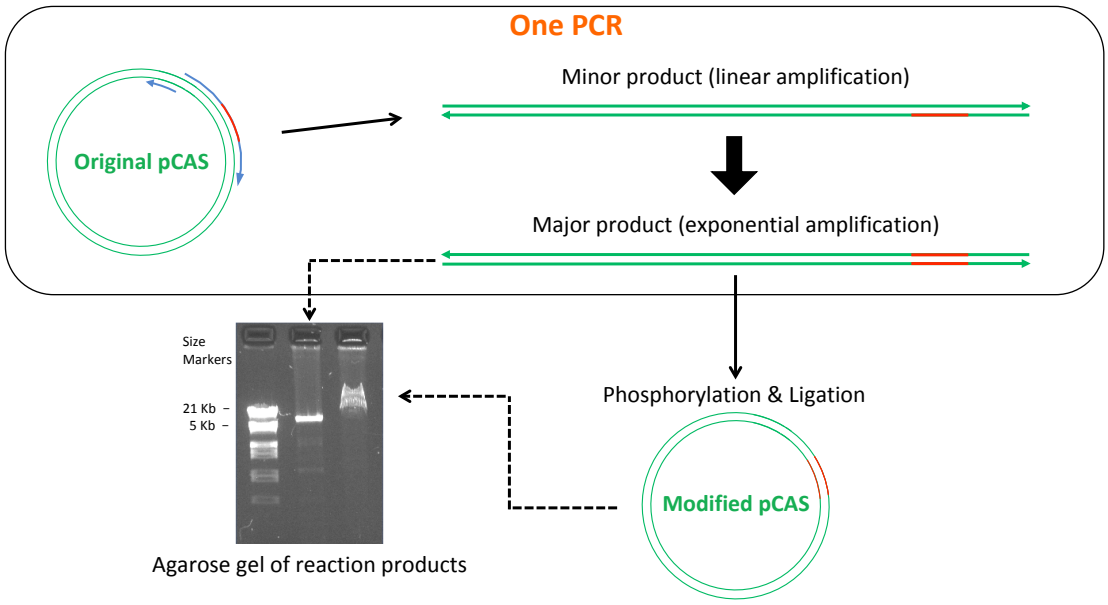

Figure 3. Inverse PCR is fast and efficient in modifying CRISPR guide sequences. Drawings are not to scale and primer sizes (blue rounded arrows on original pCAS) are exaggerated relative to the size of the plasmid (green double lines). The modified guide sequence is colored orange on primers and plasmids. Components and events in the single PCR reaction are enclosed within the rounded rectangle at the top. Either one of the two possible primer arrangements on the original pCAS can be chosen to create the same modification of the guide RNA. The figure depicts only one primer arrangement. The 5' nucleotide of the 60 base-long GuideRNA primer and of the 20 or 27 base-long Extend primer (Table I) correspond to adjacent nucleotides on the plasmid sequence, producing full-length, blunt-ended, linear products that are directly phosphorylated, ligated, and used in transformation. Sub-nanogram quantities of the original 8.7 Kb plasmid can yield micrograms of modified plasmid as shown by the gel image. The very large excess of modified plasmid over the amounts of original and minor product DNA bypasses the need to eliminate the minor DNAs before transformation, as 50% or more of the *E. coli* transformants will have the desired guide sequence.

self-complementary dramatically increases product yield and eliminates the need for DpnI treatment (Fig. 3). One of the two is 60 bp long and is the mutagenic primer (GuideRNA primers in Table 1), designed according to the guidelines in RYAN *et al.* (2016) to contain the desired 20-bp guide sequence flanked on both sides by 20-bp sequences homologous to the plasmid. The other is a normal, shorter PCR primer not overlapping with but immediately adjacent to the long primer on

Name	Sequence 5' to 3'	Function
CgSSint1_SS2F	AGGGCCCATTCGGGTCTTGTAATTGGAATGAGTACAATGTAAATACCTTA**GTATGTCAAATAATCCTTTTC**	To obtain intron insertion fragment from *C. grayi*
CgSSint1_SS2R	GGAATTACCGCGGCTGCTGGCACCAGACTTGCCCTCCAATTGTTCCTCGT**CTATTAATGATGTTAGTAATG**	
CgSSint1_LS7F	AGTCCCTCGGAATTTGAGGCTAGAGGTGCCAGAAAAGTTACCACAGGGAT**GTATGTCAAATAATCCTTTTC**	
CgSSint1_LS7R	AGAATCAAAAAGCAATGTCGCTATGAACGCTTGACTGCCACAAGCCAGTT**CTATTAATGATGTTAGTAATG**	
GuideRNA_SS2R	GCTATTTCTAGCTCTAAAAC**CGTTAAGGTATTTACATTGT**AAAGTCCCATTCGCCACCCG	To modify the pCAS guideRNA sequence
GuideRNA_LS7F	CGGGTGGCGAATGGGACTTT**AAAGTTACCACAGGGATAAC**GTTTTAGAGCTAGAAATAGC	
GuideRNA_LS7ncF	CGGGTGGCGAATGGGACTTT**CCACAAGCCAGTTATCCCTG**GTTTTAGAGCTAGAAATAGC	
pCAS_ForwExtend	AAGTTAAAATAAGGCTAGTCCGTTATC	
pCAS_RevExtend	AAGGTGTTGCCCAGCCGGCG	
YrDNA10F	GCTCGTAGTTGAACTTTGGGCC	Yeast colony PCR
YrDNA18R	GGCCCAAAGTTCAACTACGAGC	
Cg28S_F2	CAGTGTGAATACAAACCATGAAAGTG	
Cg28S_R1	CCAACGCTTACCGAATTCTGCTTCGG	
PCR Control F	ACGGCGCGAAGCAAAAATTAC	To check for plasmid loss
PCR Control R	TGCCCGACATTATCGCGAG	
GuidePrimerSS2F	ACAATGTAAATACCTTAACG	Primers specific for guideRNA sequences
GuidePrimerLS7R	GTTATCCCTGTGGTAACTTT	
GuideSeq	CGGAATAGGAACTTCAAAGCG	Sequencing primers
pCAS_Seq_R	AAGCACCGACTCGGTGCCAC	
pCAS_Seq_R2	GAGGCAAGCTAAACAGATCTC	
Y-SSUqF2	CACCAGGTCCAGACACAATAAG	qPCR primers
Y-SSUqR2	CAGACAAATCACTCCACCAACTA	
Y-Act1qF4	CGTCTGGATTGGTGGTTCTATC	
Y-Act1qR4	GGACCACTTTCGTCGTATTCTT	

Table 1. Primers used in this study. The 3' end sequences bolded in the first set of primers anneal to the 5' and 3' end regions of the intron respectively. The T in red is a mismatch designed to modify the 5' splice site. The fifty 5' bases match the yeast rDNA flanking the Cas9 cut site. The twenty bases bolded in the second set of primers are the guide sequences for Cas9.

the plasmid sequence (Fig. 3). Using the inverse PCR method, we constructed three modified pCAS plasmids, pCAS_SS2, pCAS_LS7, and pCAS_LS7nc with, respectively, primer pairs GuideRNA_SS2R and pCAS_ForwExtend, GuideRNA_LS7F and pCAS_RevExtend, and GuideRNA_LS7nc and pCAS_RevExtend (Table 1). The three, 10 µl inverse PCR reactions each contained 5.1 µl dH_2O, 2 µl Phusion buffer (NEB), 0.5 µl of each 10 µM primer, 0.8 µl dNTPs, 2.5 mM each, 1 µl (1 ng) pCAS, 0.1 µl Phusion HF DNA Polymerase (NEB). It is important to use the relatively high dNTP concentration in the reaction (200 µM each) recommended by the manufacturer to avoid unwanted deletions and mutations around the plasmid ligation junction. At lower dNTP concentrations the 3'>5' exonuclease activity of Phusion polymerase increases and could damage primer and amplicon ends. Thermocycling conditions were as described in Table 2A. The linear PCR product was 5' phosphorylated at 37°C for 30 min in a 20 µl reaction (NEB): 15 µl dH_2O, 2 µl T4 DNA Ligase buffer, 2 µl PCR product, 1 µl T4 Polynucleotide kinase. For blunt-end ligation, 1 µl T4 DNA Ligase (NEB) was added, and the reaction was incubated at 19°C for 2 hours.

Competent *E. coli* (strain DH10B) were transformed with each of the three plasmids and plated on LB-kanamycin medium. Colony PCR was first used to screen 10-20 transformants for the

likely presence of the correct guide sequence, followed by sequencing for confirmation. The primers used for colony PCR (Table 1) were GuidePrimerSS2F, and pCAS_Seq_R for plasmid pCAS-SS2, GuidePrimerLS7R and GuideSeq for plasmid pCAS-LS7, and GuideSeq and pCAS_Seq_R2 for plasmid pCAS-LS7nc. For the first two plasmids, one primer (GuidePrimerSS2F or GuidePrimerLS7R) was specific for the guide sequence so that a PCR product would form only in presence of the correct guide sequence. Both primers used for plasmid pCAS-LS7nc were flanking the guide sequence, whose correctness was then directly confirmed by sequencing. Typically, the 10 µl colony PCR contained 4.1 µl dH_2O, 5 µl Apex Taq DNA Polymerase Master Mix solution, 0.2 µl of each 10 µM primer, and 0.5 µl of a diluted *E. coli* suspension. The diluted suspension was obtained by transferring into 10 µl dH_2O about 0.1 µl of cells picked up with a sterile loop from an *E. coli* colony. PCR conditions were as described in Table 2C. Plasmids were isolated from transformants using a standard alkaline lysis procedure (BIRNBOIM AND DOLY 1979) and cleaned with a QIAquick PCR purification kit. The presence of the correct gRNA sequence on the isolated plasmid was confirmed by sequencing using forward primer GuideSeq and either pCAS_Seq_R or pCAS_Seq_R2 as the reverse primer.

	A.	
	Temperature	**Time**
	98°C	30 sec
30 cycles	98°C	10 sec
	58°C	1 min
	72°C	4 min
	72°C	2 min

	B.	
	Temperature	**Time**
	98°C	30 sec
34 cycles	98°C	10 sec
	55°C	30 sec
	72°C	10 sec
	72°C	5 min

	C.	
	Temperature	**Time**
	94°C	4 min
39 cycles	94°C	30 sec
	50°C	30 sec
	72°C	15 sec
	72°C	7 min

	D.	
	Temperature	**Time**
	95°C	5 min
39 cycles	95°C	30 sec
	60°C	30 sec
	72°C	2 min

Table 2. Thermocycling conditions referred to in the text.

Intron PCR

Cladonia grayi DNA was isolated as described in ARMALEO AND MAY (2009). The 57-bp intron we chose for transfer into yeast rDNA was amplified from *C. grayi* DNA with two PCR primer pairs, CgSSint1_SS2F and CgSSint1_SS2R for insertion into the 18S (SSU) sequence, or CgSSint1_LS7F and CgSSint1_LS7R for insertion into the 25S (LSU) sequence (Fig. 3 and Table 1). Each 25 µl PCR contained 17.3 µl dH_2O, 5 µl Phusion Buffer, 0.1 µl of each 100 µM primer, 0.5 µl of dNTPs, 2.5 mM each, 1 µl (5 ng) *C. grayi* DNA, 1 µl Phusion HF DNA Polymerase. PCR conditions are listed in Table 2B. Each PCR product was cleaned with a QIAquick PCR purification kit and used directly for yeast co-transformation with the appropriate pCAS plasmid variant (next section). Each 157-bp PCR fragment contained the intron flanked by homologous 50-bp segments to either the small or the large subunit rDNA of yeast, to direct integration by HDR (Fig. 3). The branchpoint and 3' splice site sequences of

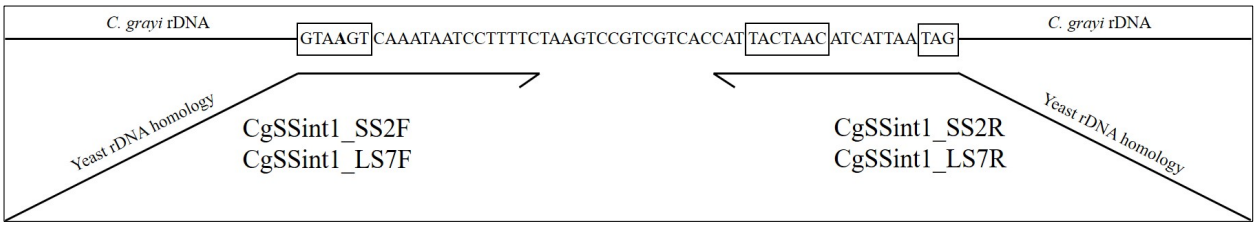

Figure 4. Incorporation of a C. grayi intron into a PCR fragment for integration into yeast rDNA. The top line shows the intron sequence within *C. grayi* rDNA. From left to right, boxes highlight the 5' splice site, branchpoint, and 3' splice site consensus sequences, respectively. The bolded A in the 5' splice site was changed to a T through primer CgSSint1_SS2F or CgSSint1_LS7F. The primer regions annealing to the intron are drawn parallel to the intron, with arrowheads indicating the 3' ends. Tilted are the 50-bp regions homologous to yeast rDNA, which allow intron integration by HDR into yeast rDNA cut by Cas9 within the homologous regions. Not drawn to scale.

the lichen intron match the most common consensus sequences in yeast (KUPFER *et al.* 2004), but the 5' splice site, GUAAGU, corresponds to a less frequent yeast version. To make the 5' splice site identical to the most common consensus in yeast, GUAUGU (KUPFER *et al.* 2004), we introduced into the forward primer a one base A>T mismatch with the original lichen sequence (Fig. 4 and Table 1).

Yeast transformations, colony PCR, test of plasmid loss

Single intron insertion yeast strains MSS2 and MLS7 were obtained from wildtype strain YJ0 by cotransformation, respectively, with pCAS-SS2 + SSU intron fragment and pCAS-LS7nc + LSU intron fragment. The double insertion strain M-d was obtained from strain MSS2 by cotransformation with pCAS-LS7 + LSU intron fragment. We also performed transformations using plasmids pCAS-SS2 or pCAS-LS7nc each by itself, to screen for small mutations around the Cas9 cut sites rather than intron insertions. The protocol by RYAN *et al.* (2016) was followed for competent cell preparation and transformation. In each co-transformation, 100 µl competent cells were combined with 1 µg pCAS plasmid derivative and 5 µg intron fragment. Transformants were selected on G418 YEPD plates incubated at 30°C. Many transformants were slow growing and colonies became visible after 3-4 days. Individual transformants were screened for intron insertion or for small mutations by colony PCR using primers flanking each expected insertion/small mutation site and sequencing of PCR products. For PCR, 0.01-0.05 µl cells from each yeast colony were transferred to a microfuge tube containing 50 µl TE, 0.1% SDS and 50 µl of 0.3 mm glass beads, vortexed and heated for 4 minutes at 90°C, and 1 µl lysate was diluted into 4µl TE. Typically, the 10 µl PCR contained 4.4 µl dH_2O, 5 µl Apex Taq DNA Polymerase Master Mix, 0.2 µl each of 10 µM primer (YrDNA10F/YrDNA18R for the small subunit and Cg28S_F2/Cg28S_R1 for the large subunit, Table 1), and 0.1 µl of the diluted yeast lysate. Thermocycling conditions were as described in Table 2D. After prolonged growth in YEPD lacking G418, yeast transformants were checked for plasmid loss using the same colony PCR protocol with plasmid-specific primers PCR Control F and PCR Control R (Table 1). All yeast mutant strains used in the experiments had lost the Cas9 plasmid.

RNA extraction, cDNA preparation

To demonstrate intron splicing, total RNA was extracted from the MSS2 transformant, bearing the intron in the 18S rRNA repeats. A 10 ml overnight culture was pelleted, the pellet was frozen with liquid N_2 and thoroughly ground in a mortar with liquid N_2. The ground cells were resuspended in 1.5 ml of a 0.88:0.22 mix of Lysis solution and Plant RNA isolation aid solution from the RNAqueous Total RNA Isolation Kit (ThermoFisher Scientific). Subsequent steps

followed the RNAqueous kit protocol. Isolated RNA was quantified by NanoDrop (ThermoFisher Scientific) and quality was assessed by agarose gel electrophoresis. Using Superscript III RT (ThermoFisher Scientific), reverse transcription was performed at 50°C for 120 min in a 25 µl volume with 100 ng RNA and the reverse primer YrDNA18R (Table 1), whose 5' end is 111 bases downstream from the intron insertion site. After completion of the reaction, RNA was hydrolyzed by adding NaOH to 250 mM concentration. The cDNA was subsequently used as template in PCR using primers YrDNA10F and YrDNA18R (Table 1). PCR conditions were as described for yeast colony PCR (Table 2D). The PCR fragment sizes with and without intron are 290 and 233 bp respectively. Correct splicing was confirmed by sequencing.

Relative rDNA copy number determination

We used qPCR to determine the relative number of rDNA copies in the mutants *vs*. the wildtype strain. Each strain was grown in 10 ml YEPD at 30°C to early stationary phase, and DNA was extracted (HOFFMAN AND WINSTON 1987). DNA concentration was estimated by Nanodrop (ThermoFisher) and fine-tuned by measuring band intensity on gels. The relative change in rDNA copy number in MSS2 and MLS7 relative to YJ0 was assessed (Additional File 1) with the ΔΔCt method as modified by PFAFFL (2001) to allow for different amplification efficiencies between reference and target gene. As target we used a section of SSU rDNA, amplified with primers Y-SSUqF2 and Y-SSUqR2, for an amplicon size of 102 bp. As reference we used the single-copy ACT1 gene, amplified with primers Y-Act1qF4 and Y-Act1qR4, for an amplicon size of 87 bp. In each of two replicate qPCR experiments, each DNA was tested in triplicate with the SSU primers and with the ACT1 primers. Reactions were run in 96-well plates in a Bio-Rad Chromo 4 machine, with Opticon Monitor software version 3.1. Each 15 µl reaction contained 6.17 µl H_2O, 0.03 µl Rox dye (50 nM), 0.15 µl SybrGreen (1:100), 7.5 µl Apex polymerase mix, 0.075 µl F primer (10 µM), 0.075 µl R primer (10 µM), 1µl DNA (0.1 ng/µl). Cycling conditions (°C/seconds): start cycle 95/60; 40 cycles 95/30 – 56/30; end at 12°C. Amplification efficiencies, 1.55 for SSU and 1.47 for ACT1, were calculated by the Opticon Monitor software.

Growth Assay

Growth assays were done on YJ0, MSS2, MLS7, and M-d. For each strain, a fresh agar plate culture was used to prepare a liquid suspension in YEPD with a concentration between 10^3-10^5 cells/ml, assuming an OD_{600} of 1 = 3 x 10^7 cells/ml. Twelve 150 µl aliquots of the suspension were loaded in three groups (biological replicates) of four technical replicates on two adjacent columns of a 96-round-bottom well plate. To generate growth curves, an automatic plate reader (Tecan) was used to record the OD_{600} at 30°C every 15 minutes over a period of 96 hours. The plate was shaken for 60 seconds before each measurement.

Desiccation Assay

We modified in two ways the method by WELCH AND KOSHLAND (2013). Desiccation was performed in the flow hood rather than in the speedvac and colonies were counted on agar plates rather than directly in the liquid culture wells. All procedures were sterile and media were YEPD. Growth was at 30°C, and liquid cultures were shaken at 255 rpm. Fresh overnight liquid cultures of YJ0, MSS2, MLS7 and M-d were diluted to an OD_{600} between 0.1 and 0.25 and grown to 0.5 OD_{600}. For each strain, duplicate 1 ml aliquots were pelleted in microfuge tubes. Pellets were resuspended in 1 ml of H_2O, re-pelleted, and all the water was carefully removed with a pipette. One of the duplicate aliquots (designated as "undesiccated") was immediately resuspended in 100

µl medium, serially diluted 10x in a column of a 96-well plate, and three 5 µl replicates from each dilution were spotted on an agar plate. The other duplicate aliquot ("desiccated") was laid against the sterile air flow in a laminar flow hood to dry for 24 hours, resuspended in 100 µl medium, serially diluted and plated the same way as the undesiccated replicate. The number of survivors in each case was estimated by counting colonies at the highest countable dilutions and extrapolating to the number of viable cells in the starting suspension. Desiccation resistance was defined as the fraction of viable cells in the desiccated *vs.* undesiccated sample. Three to six biological repeats were performed with each strain. P-values were calculated with a two-sided Student's t-test.

Microscopy

Budding frequency was measured in a haemocytometer with samples from mid-log phase cultures in YEPD liquid medium. For photography, diluted cell suspensions were plated on YEPD and incubated at 30ºC. The YJ0 wildtype was photographed after overnight growth, the mutants after 48-72 hrs. A 1.5 x 1.5 square of agar was cut out of the plate, placed onto a microscope slide, and 10 µl water were placed on the surface followed by a cover slip. The water improved spreading of the cells from the incipient colonies and prevented air pockets under the coverslip.

Intracellular trehalose measurement

The method was essentially as described by TAPIA *et al.* (2015), and GIBNEY *et al.* (2015). Each strain was grown at 30ºC in YEPD liquid medium to an OD_{600} between 0.3 and 0.5. A volume containing 10^7 cells was harvested, cells were pelleted, resuspended in 2 ml ice-cold water and re-pelleted. Each pellet was resuspended in 250 µl of 0.25 M sodium carbonate, and the suspension was transferred to a 2-ml screwcap tube and stored a -80ºC until trehalose extraction. Trehalose was extracted from cells by incubating the tightly sealed samples at 98ºC for 4 hours, with occasional mixing. Samples were stored at -20ºC. For trehalase treatment, each 250 µl sample was mixed with 150 µl of 1M acetic acid and 600 µl 0.2 M sodium acetate, cell debris were pelleted, and 250 µl were removed from the top of the sample and stored at -20ºC (untreated control). To the remaining 750 µl, 0.35 µl trehalase (Megazyme, at 4.2 units/µl) were added for a final concentration of 2 units/ml, and reactions were incubated overnight at 37ºC on a rotating wheel. After pelleting cell debris, the supernatant (750 µl) was transferred to a new tube to be assayed for glucose either immediately or, if convenient, after storage at -20ºC, using the Glucose (GO) assay kit from Sigma Aldrich. For each assay, 220 µl of sample were mixed with 440 µl kit reagent in a 15-ml glass test tube, capped and incubated at 37ºC for 30 minutes, and 440 µl of 6M sulfuric acid were added in a fume hood with a 1-ml glass pipette. Absorbance at 540 nm was measured in 1-ml plastic cuvettes. The untreated controls were used to measure background glucose, water samples were used as blanks and glucose standards to determine concentration.

Results

CRISPR is effective in introducing introns or base pair changes into all yeast rDNA repeats.

Genetic manipulations of lichen fungi are in their infancy (WANG *et al.* 2020; LIU *et al.* 2021). Therefore, we tested the effects of lichen rDNA introns in the model fungus *S. cerevisiae*, whose rDNA is normally intronless. We transformed yeast with a 57 base-pair spliceosomal intron from the rDNA of the lichen fungus *Cladonia grayi* (ARMALEO *et al.* 2019). The splicing signals overlap with those of yeast mRNA introns (Fig. 4), and thus are expected to be recognized by yeast

spliceosomes. CRISPR-Cas9 technology was seen as the only available way to simultaneously insert the intron into 150 repeats of yeast rDNA (CHIOU AND ARMALEO 2018; SANCHEZ *et al.* 2019) because of the powerful selection of CRISPR against unmodified rDNA. Our method was developed to insert introns into the 18S and 25S rRNA genes by Homology Directed Repair (HDR), but we list here for the record also the base pair substitutions produced through Non-Homologous End Joining (NHEJ) during this work (Additional File 2).

Three intron-bearing mutants were constructed, with the intron stably inserted either in all copies of the 18S (SSU) gene, of the 25S (LSU) gene, or of both. The selected yeast insertion sites corresponded to two *C. grayi* intron sites and had appropriately located PAM sequences (Fig 5). Intron insertions were obtained by cotransformation of yeast with a Cas9-gRNA plasmid and the

Figure 5. Intron insertion sites in the 18S and 25S rRNA genes of yeast. Only sense-strand sequences are shown, 5' ends on the left. PAM sequences are marked red. The intron is colored orange and its insertion points by HDR are indicated by the blue-dotted brackets. The vertical dash marks the nucleotide 5' to the Cas9 cut site on the rDNA sequence and the numbers indicate the corresponding positions in the mature rRNA.

corresponding intron containing fragment. Single intron insertion mutants MSS2 and MLS7 contain the intron in the 18S or 25S rRNA gene at positions 534 or 2818 respectively (Fig. 5). The double insertion mutant M-d contains the intron at those positions in both genes. All mutants were verified by PCR (Fig. 6) and sequencing; additionally, correct splicing in MSS2 was confirmed by sequencing the mature rRNA. Regardless of whether we inserted introns or produced base-pair mutations around the Cas9 cut sites, the introduced changes appear to involve all repeats as suggested by the absence of heterogeneous peaks at the mutation sites in the sequencing

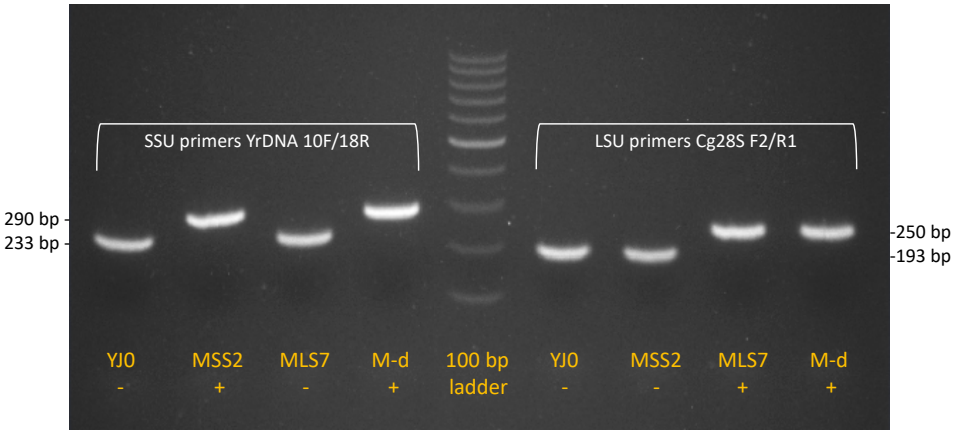

Figure 6. Agarose gel showing intron location in the yeast strains. Primer pairs (white lettering) flanking each intron insertion site were used for PCR with the DNA from the four strains (orange lettering). For each primer pair, the sizes (base pairs) of the fragments with or without the intron are indicated on the side. Intron absence/presence in each fragment is labeled -/+. The sizes indicate that the wildtype strain YJ0 has no introns, MSS2 has the intron only in the SSU gene, MLS7 has the intron only in the LSU gene, M-d has the intron in both genes. The lanes with the intron fragments contain no discernible trace of intronless fragments, suggesting that the introns spread through all rDNA repeats.

chromatograms (Additional File 2) and by the absence of intronless bands in PCRs spanning the intron insertions (Fig. 6). In addition, rDNA introns are stably inherited, which also suggests that no intronless repeats were left to act as recombination seeds and restore the wildtype intronless configuration. Spreading an intron to all yeast rDNA repeats was also achieved by Volker Vogt's group (MUSCARELLA AND VOGT 1993; LIN AND VOGT 1998) with a method foreshadowing our use of CRISPR-Cas9 to the same end: to study intron endonucleases, they introduced functional group I rDNA introns from *Physarium polycephalum* or *Tetrahymena thermophila* into yeast rDNA.

Small nucleolar RNAs may interfere with Cas9 when targeting rDNA

Despite two attempts, CRISPR-mediated intron insertion into the rDNA of the YJ0 wildtype using the large subunit guide sequence LS7 (matching the sense strand) failed. It was however successful when we used the LS7nc guide sequence (matching the template strand at the same location). This made us suspect that an endogenous yeast sequence serendipitously complementary to the LS7 guide RNA could have inhibited LS7-Cas9. A small nucleolar RNA (snoRNA) was considered a likely culprit. During yeast rRNA synthesis and ribosome assembly, a number of specific ~100- to 1000-nucleotide long snoRNAs bind as ribonucleoprotein complexes to complementary sequences on the rRNA, leading to post-synthetic nucleotide modifications in those sequences (DUPUIS-SANDOVAL *et al.* 2015). A snoRNA (snR38) with an 11-base complementarity to the 3' terminal region of the LS7 guide sequence (Fig. 7A) is in fact listed in the yeast snoRNA database (https://people.biochem.umass.edu/fournierlab/snornadb/main.php). Although we do not demonstrate this directly here, the likelihood that snR38 inhibited Cas9 by binding to LS7 is supported a) by the fact that the complementarity is in the snoRNA region that is meant to bind directly to rRNA to methylate it, b) by the successful insertion of the intron at the same position when using the LS7nc guide which is not complementary to snR38 (Fig. 7A and B), and c) by the

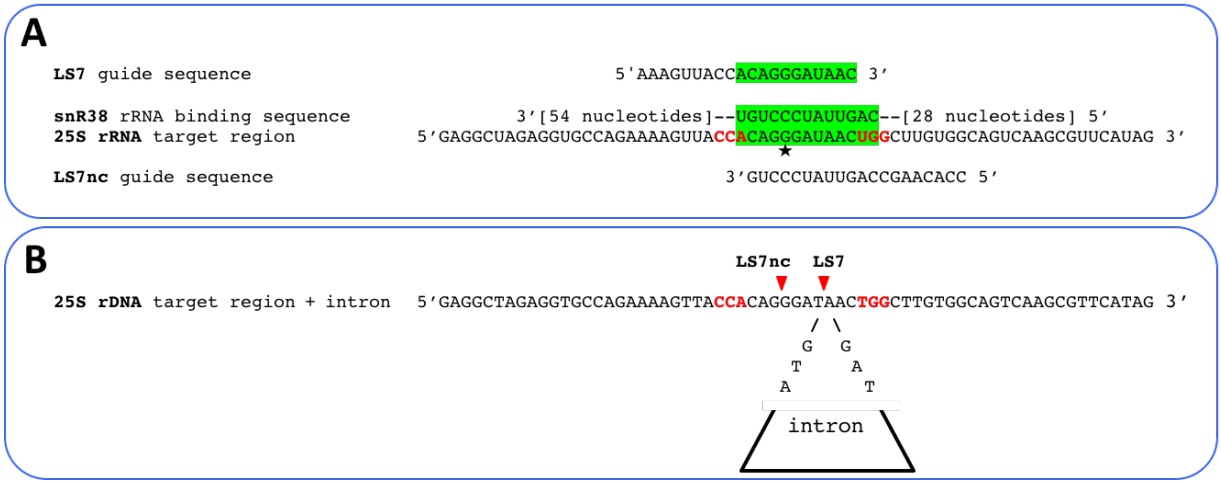

Figure 7. Cause of the likely inhibition of Cas9 by snR38, and intron targeting to the LSU gene. **A.** Complementary binding between the RNA-binding region of snR38 and the LS7 guide RNA is likely to have inhibited the Cas9-LS7 complex. RNA complementary regions are highlighted green; nucleotides corresponding to a PAM sequence on either strand are in red; the star marks rRNA nucleotide 2815, targeted for O-methylation by snR38; Cas9 was not inhibited when used with guide RNA LS7nc, which could not bind to snR38. **B.** The intron was inserted at the LS7 site using LS7nc guide RNA. Red arrowheads indicate the Cas9 cut sites (at positions 2814 for LS7nc and 2818 for LS7) corresponding to the two opposite-strand PAM sites (in red). While LS7nc directed Cas9 to cut the site on the left, homology directed repair integrated the intron in the rDNA in correspondence of the LS7 site at position 2818, where the intron was located in the PCR fragment used in co-transformation.

absence of a snoRNA complementary to the SS2 guide sequence which mediated the successful insertion of the intron into the SS2 site. Fig. 7B also shows that the exact insertion point is determined by the placement of the intron within the co-transforming PCR fragment, even if it is a few bases removed from the actual Cas9 cut site.

Introns decrease rDNA copy number, inhibit growth, and modify cell morphology

To assess whether intron presence affects rDNA copy number, we used the ΔΔCt qPCR method by (PFAFFL 2001) to determine the relative number of rDNA copies in mutants *vs.* wildtype. Copy numbers in each of the single-intron mutants MSS2 and MLS7 decreased to about 53% of the YJ0 wildtype (Additional File 1). The qPCR data from the double-intron mutant M-d were uninterpretable for unclear reasons. The intron-bearing mutants produced small, slow-growing colonies and their growth rates in liquid culture were 4-6 times slower than that of YJ0 (Fig. 8). It is noteworthy that the single insertion in the LSU region caused a much stronger growth inhibition than one in the SSU region, pointing to the importance of intron context and to the dominance of the 60S subunit assembly in regulating the overall assembly. The slowdown appears to lengthen the cell cycle in G1, as the strains' budding frequency is lowered from 65.6% in the wildtype YJ0 to 27.4% (MSS2), 43% (MLS7), and 39.7% (M-d). On average, cells of the intron-bearing strains are larger than those of the wildtype. The cell morphology of MLS7 and M-d is also frequently abnormal (Fig. 9) and may have inflated the bud counts in these strains.

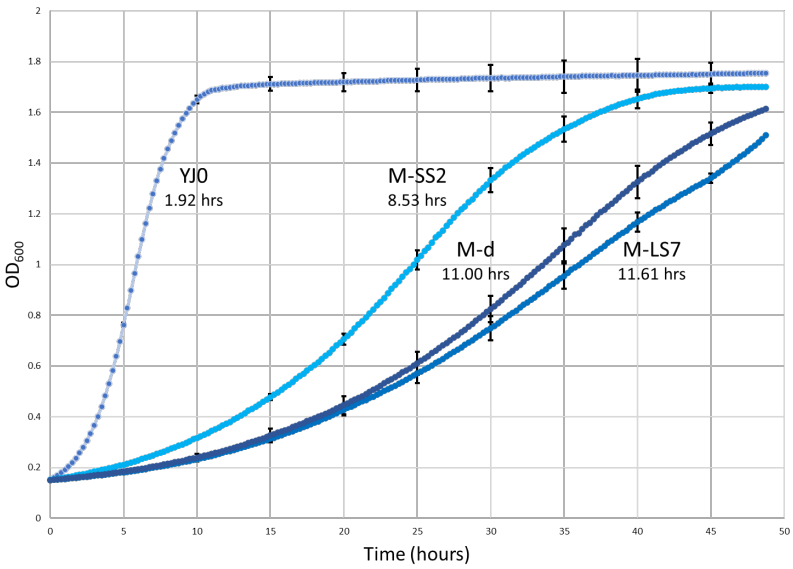

Figure 8. Growth curves for the four strains. Curves represent the means of three biological replicates and four technical replicates for each strain. Bars represent the SD. The numbers next to the curves are the doubling times for each strain.

Introns enhance desiccation tolerance in *S. cerevisiae*

We measured desiccation tolerance in the wildtype and the three intron-bearing mutants using a method modified from WELCH AND KOSHLAND (2013). Each strain was grown to mid-log phase, two identical samples were removed, and one was subjected to desiccation while serial dilutions of the other were plated. One day later the desiccated sample was resuspended and serial dilutions were plated. Desiccation tolerance (Fig. 10) for each strain is expressed as the ratio of live cells (scored as colonies) in desiccated *vs.* undesiccated samples of that strain. Fig. 10A shows the resistance of individual biological replicates. Three biological replicates were assayed for YJ0 and

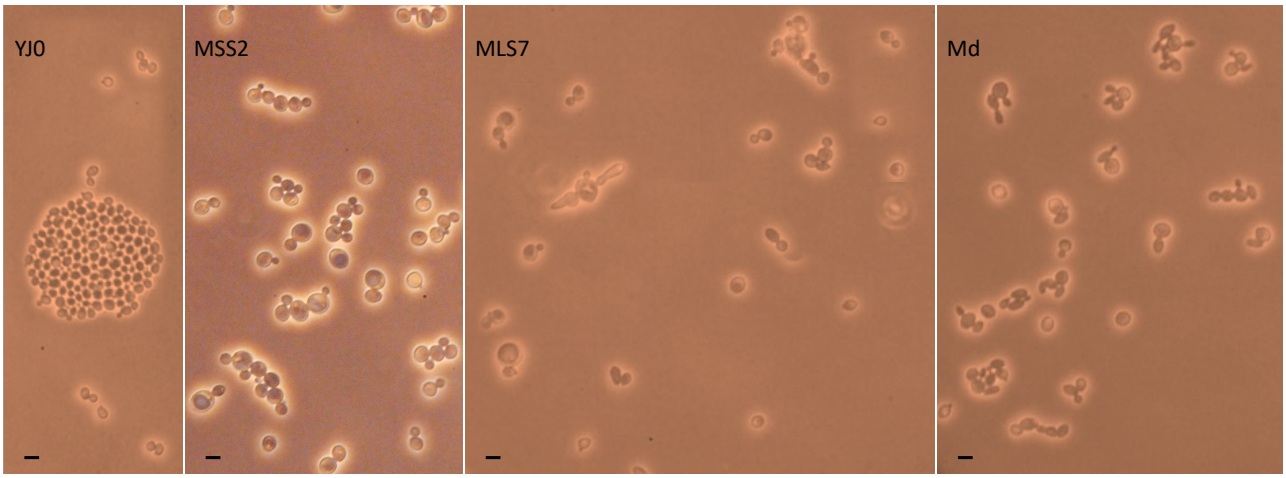

Figure 9. Cell size and morphology. Cells were photographed growing on the surface of freshly seeded agar plates. Bar = 10μ. Intron-bearing cells are on average larger than the YJ0 wildtype cells. Several MLS7 and Md cells have aberrant morphologies. Due to its faster growth, YJ0 quickly forms many incipient colonies, one of which is visible here.

M-d, and five and six biological replicates were assayed for MSS2 and MLS7, respectively. The variation between replicates might be due to small between-sample differences in drying speed and/or to the stochastic behavior of the biochemical networks underlying stress tolerance (see Discussion). Fig. 10B shows the same data plotted as averages of the biological replicates. For YJ0, the average absolute survival was 1.5 x 10^{-5}. The average absolute (and relative) survival ratios for

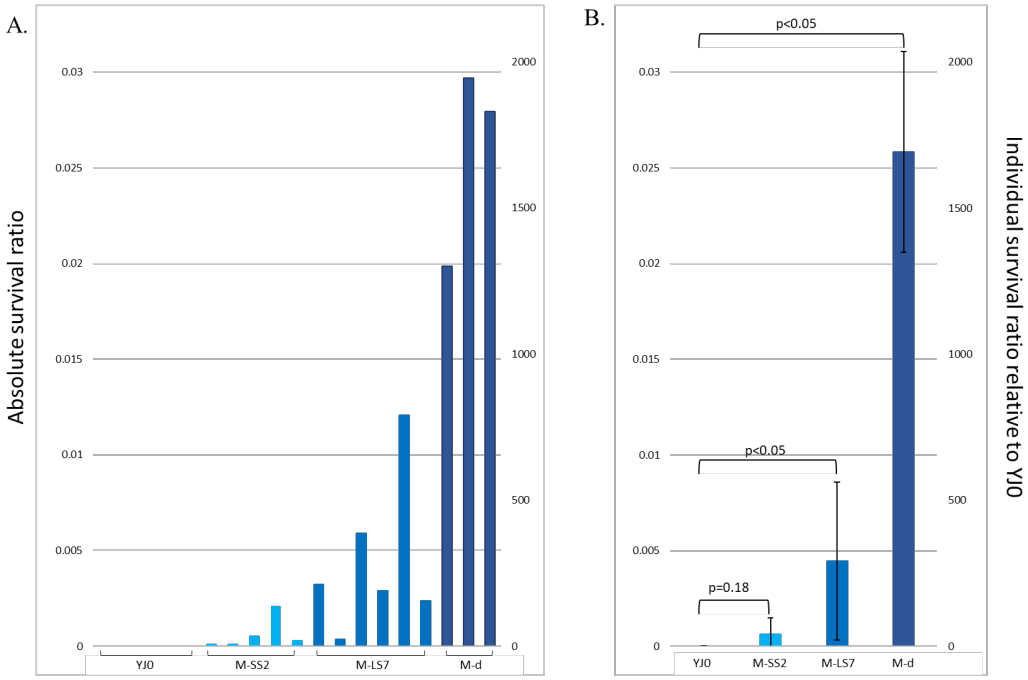

Figure 10. Desiccation resistance of the four strains. The Y axes are the same in both panels. Absolute survival ratios represent the fraction of cells surviving desiccation within each strain. Relative survival ratios represent each strain's resistance relative to that of the YJ0 wildtype. **A.** Resistances of individual biological replicates. **B.** Same data averaged over biological replicates; SD in black; brackets indicate p values for mutant *vs*. wildtype ratios.

.
MSS2, MLS7, and M-d were $6.3x10^{-4}$ (42), $4.5x10^{-3}$ (300), and $2.6x10^{-2}$ (1700). The position and number of introns affects desiccation resistance. Paralleling their effect on growth (Fig. 8), MLS7 with the intron in the large subunit is more desiccation resistant than MSS2 with the intron in the small subunit. M-d, the strain with introns in both subunits, is the most resistant.

Introns induce trehalose biosynthesis in the double mutant

In some organisms, including yeast, intracellular concentrations of the disaccharide trehalose are positively correlated with desiccation tolerance (KOSHLAND AND TAPIA 2019). We therefore measured whether intracellular trehalose accumulates in our mutants during normal growth. The procedure involves extraction of trehalose from a fixed number of mid-log phase cells grown in YEPD medium followed by trehalase treatment to split trehalose into its two glucose constituents, and finally by a colorimetric assay that measures glucose concentration. The results (Fig. 10) indicate that trehalose was undetectable not only in the YJ0 wildtype, but also in the single-intron mutants MSS2 and MLS7, despite their increased desiccation tolerances. Trehalose increased to detectable levels only in the M-d strain. M-d carries two introns, one per subunit in each rDNA gene copy, and displays the highest desiccation tolerance (Fig. 9).

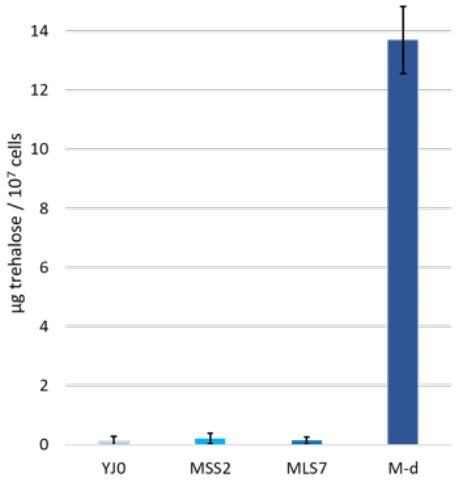

Figure 11. Intracellular trehalose in the four strains. Amounts are expressed $/10^7$ cells /ml of assay. For each strain, the SD is calculated on 9 samples (three biological replicates, each with three technical replicates).

Discussion

Since the discovery of lichen rDNA introns decades ago (DEPRIEST 1993a), the functional reasons for their anomalies have not been addressed. To test whether these introns affect slow growth and desiccation tolerance in lichens, we modeled in yeast a lichen-like nuclear rDNA intron arrangement using CRISPR to insert a lichen spliceosomal rDNA intron at one or two positions into each rDNA repeat (Figs. 4 and 5). Bending the general rule that spliceosomes operate only on Polymerase II transcripts, the yeast machinery successfully removed the lichen spliceosomal introns from the Polymerase I rRNA transcripts, allowing us to test in yeast the behavior of lichen rDNA introns. The next three background sections describe our rationales to interpret the experimental results and connect them to what we think happens in lichens.

1. The inability of lichen rDNA introns to self-splice inhibits both rRNA processing and ribosomal protein synthesis

Excision of degenerate group I introns must require a specific and as yet unidentified machinery in lichen fungi. How could it have evolved? Despite lacking sequences needed for self-splicing, lichen group I introns appear still able to fold into tertiary structures resembling the original ones (DEPRIEST AND BEEN 1992; BHATTACHARYA *et al.* 2000; BHATTACHARYA *et al.* 2002; HAUGEN *et al.* 2004b). It is therefore possible that, while progressively removing catalytically important sections from the introns, natural selection transferred splicing capability to the maturases that originally helped those structures fold. Cloning lichen maturases could verify such a scenario.

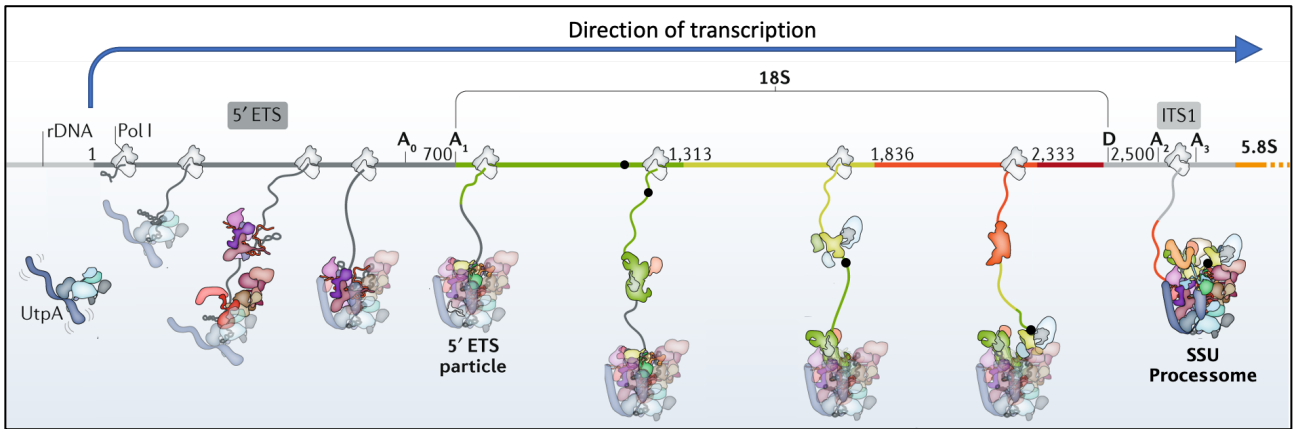

Figure 12. Visualization of how delayed intron splicing could interfere with ribosome assembly. The scheme depicts early nucleolar phases of the cotranscriptional assembly of yeast 18S pre-ribosomal particles. From the start of transcription, several assembly factors interact dynamically with the nascent rRNA, initiating ribosome construction. The grey parts of the nascent RNA correspond to the 5' ETS and ITS1, the colored parts to the mature 18S rRNA. The intron inserted into the yeast 18S rDNA is depicted as a proportionally sized black dot located on the DNA and incorporated upon transcription into the growing pre-ribosomal particle. The bulky and relatively slow spliceosome (not depicted here, but comparable in size to the processome) removing the intron is expected to interfere with ribosome assembly, delaying it. We depicted the intron as persisting up to the processome stage, but we do not know when the intron is removed. A similar interference by the intron is expected to delay maturation of 25S pre-ribosomal particles (not shown). The diagram was modified from KLINGE AND WOOLFORD (2019) with permission.

Since the ribosome assembly process is highly cooperative and perturbation-sensitive (OSHEIM *et al.* 2004), we propose that the lichen machinery removing the numerous group I introns scattered throughout the nascent rRNA interferes with and delays the rapid cotranscriptional assembly of pre-ribosomal protein-RNA complexes (KLINGE AND WOOLFORD 2019), slowing rRNA processing and ribosome biogenesis. The spliceosomes removing the few spliceosomal introns from lichen pre-rRNA would have the same effect, which we model here in yeast (Fig. 12).

However, we ascribe the evolutionary permanence of two kinds of introns in lichen rDNA to the fact that the primary effect of spliceosomal introns on ribosomal assembly is different from that of group I introns. Spliceosomal introns in rRNA mostly compete with their mRNA counterparts for spliceosomal components, directly inhibiting splicing of ribosomal protein (RP) mRNAs and RP synthesis. Competition between the highly expressed intron-rich RP genes, which use the most splicing factors (ARES *et al.* 1999), and other intron-containing genes has been demonstrated in yeast (MUNDING *et al.* 2013). Even with a reduced number of rDNA genes (70 to 80), the single intron mutants would have roughly 25% more spliceosomal introns in their genome than the wildtype strain. The inhibition of RP synthesis might be deepened if these introns persist as

undegraded and linearized RNAs after splicing (MORGAN *et al.* 2019; PARENTEAU *et al.* 2019). This possibility is strengthened by the fact that the lichen introns we surveyed (namely the intron we use in our experiments (Fig. 4), the three other spliceosomal introns found in *C. grayi*'s rDNA (not shown), and those from other lichens whose sequences are shown in BHATTACHARYA *et al.* (2000), satisfy the necessary and sufficient requirement for post-splicing persistence in yeast described by (MORGAN *et al.* 2019): they all have less than 25 nucleotides between the lariat branch point and the 3' splice site.

2. Lichen rDNA introns shift the mycobiont ESR towards a state of permanent desiccation alert

In yeast, ribosomal synthesis during unstressed growth is enabled by the activity of the TOR and PKA signal transduction pathways. Environmental stress signals repress TOR/PKA, which modifies regulation of the two arms of the Environmental Stress Response (ESR) (GASCH *et al.* 2000) (Fig.13, top panel). One arm involves ~600 genes which are turned down under stress and include ribosomal biogenesis (RiBi) genes needed for rRNA, RP, and assembly factor production. The other involves ~300 genes which are induced by stress and are responsible for specific ESR defenses (iESR) like the disaccharide trehalose, chaperone proteins and redox effectors. Extreme desiccation stress quickly deprives cells of water, the most basic ingredient for any life-sustaining process. This makes it critical for desiccation-defenses to be in place before the onset of

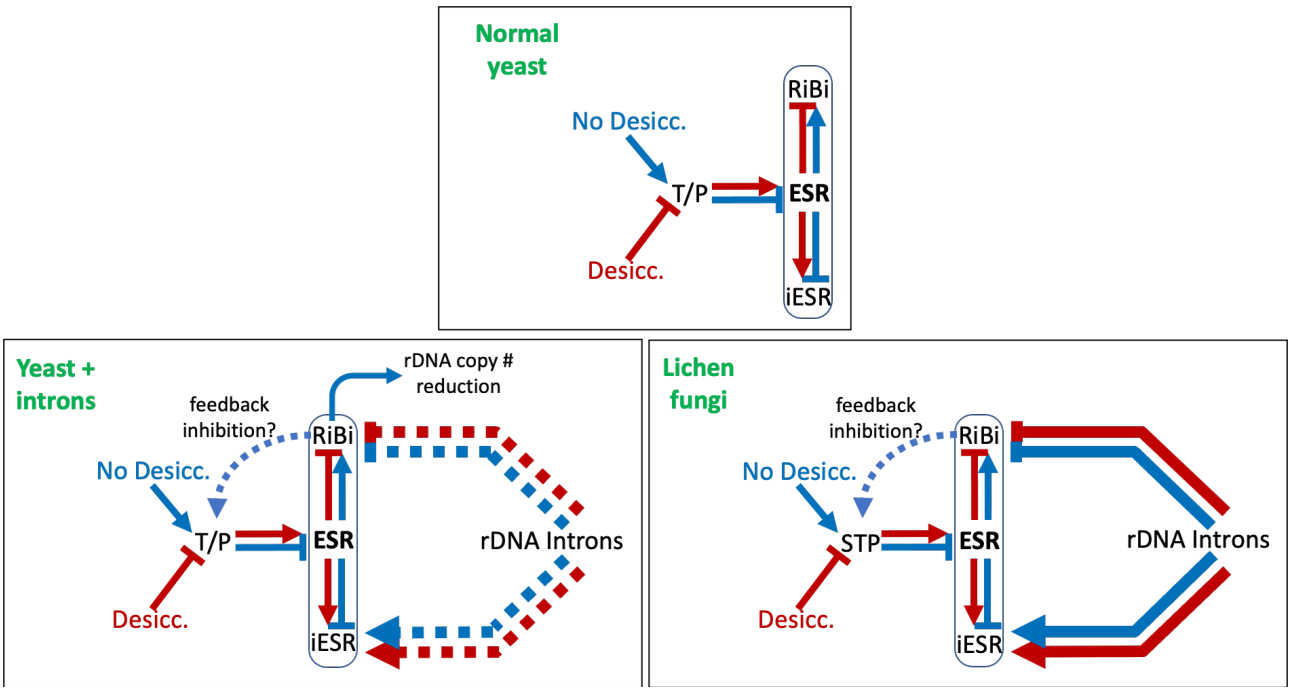

Figure 13. Working scheme of how lichen introns might affect growth and desiccation resistance. The broad features of the yeast ESR, not its details, are considered transferable to lichen fungi (see text). Metabolic effects are colored blue (unstressed growth) or red (desiccation). Arrows indicate stimulation, T-lines indicate inhibition. ESR, Environmental Stress Response; RiBi, Ribosomal Biogenesis components; iESR, induced ESR components; T/P, TOR/PKA pathways; STP, mycobiont Signal Transduction Pathways. The ESR and its two arms are enclosed in ovals. Lichen introns add to the yeast ESR new layers of regulation which keep the ESR partially active during unstressed growth and potentiate it during desiccation. Thicker lines indicate that in absence of stress, intron effects are epistatic over T/P effects. The dotted/solid intron effect lines indicate that in yeast intron effects are not spread to the entire cell population, whereas in lichens they are. Although intron effects are depicted as fully expressed in lichens during unstressed growth for simplicity (solid blue lines), mycobionts are probably able to modulate them. We define these effects as "semi-constitutive".

desiccation. Most cells in an unstressed yeast population will not express the ESR and will die when desiccated. However, due to cell-to-cell stochasticity of transcriptional, translational and post-translational network regulation (GASCH *et al.* 2017), a few unstressed cells will express the ESR and survive once water returns. This "bet-hedging" (LEVY *et al.* 2012) allows a single-celled, fast-growing organism like yeast to thrive evolutionarily, as variable subsets of the population survive under changing stresses, even if most of the population dies. Lichens, on the other hand, are slow-growing, differentiated multicellular networks of hyphae interwoven with consortia of different organisms whose adaptation to extreme and repeated moisture oscillations must ensure survival of all or most component cells, not just small subsets. We view the numerous lichen rDNA introns as a semi-constitutive defense evolved to achieve this goal by maintaining stress alertness even in absence of environmental stress signals. By semi-constitutive we mean that intron effects are not always maximal but modulated. The importance of constitutive stress-defenses in lichens has been also recognized by GASULLA *et al.* (2021). Our yeast data will be extrapolated to lichen fungi assuming resemblance of the broad outlines of their stress responses (GASCH 2007; EMRI *et al.* 2015; HAGIWARA *et al.* 2016), where extracellular signals relayed to the nucleus through signal transduction pathways lead to RiBi repression and to the activation of defensive functions (Fig. 13).

3. The repression of ribosome biogenesis is in itself protective against desiccation damage

ESR-driven RiBi repression reallocates translational resources (mRNAs) from ribosome assembly towards the specific set of resistance genes needing activation (HO *et al.* 2018). However, and this is especially relevant for desiccation stress, the RiBi downturn is also likely to be a major stress/desiccation defense in itself, based on ribosome depletion (TERHORST *et al.* 2020) and overall decreases in protein concentration. Ribosomes make up 50% of the non-liquid volume in the cytoplasm (DELARUE *et al.* 2018), and TOR inhibition can lead to a 40-50% depletion of ribosomes (DELARUE *et al.* 2018). This large decrease in ribosome number and protein synthesis reduces overall protein concentration, aggregation, misfolding (WELCH *et al.* 2013), and phase separation (DELARUE *et al.* 2018) and therefore the load on HSPs and damage to the proteome upon water loss.

Slow growth results from a three-pronged attack on ribosome biogenesis by rDNA introns

The large growth decreases in the intron-bearing yeast mutants illustrated in Fig. 8 are likely due to three main causes, all connected to the downturn of ribosome biogenesis. Two were described earlier: the interference of the splicing machinery with rRNA processing and ribosome assembly (Fig. 12), and the specific inhibition of RP and assembly factor synthesis by spliceosomal rRNA introns. The third is DNA replication stress, which probably underlies some of the observed yeast mutant phenotypes: repeat number reduction (SALIM *et al.* 2017) (Fig. 13), G1 delays, and aberrant cell morphologies (Fig. 9) (TRIPATHI *et al.* 2011). DNA stress could be due to interference of the intron splicing process with the functions of early 60S assembly factors Noc3p and Rix, which are also part of the DNA pre-replicative complex (ZHANG *et al.* 2002; DEZ AND TOLLERVEY 2004; HUO *et al.* 2012). Possibly, the gradual evolutionary insertion of introns into mycobiont rDNA allowed selection to turn partial disruptions of RiBi and DNA replication into adaptations.

Increased desiccation tolerance is a primary consequence of intron-caused RiBi repression, which is constitutive and independent of desiccation

The average desiccation survival of normal intronless *S. cerevisiae* growing in rich liquid media is ~10^{-6}. That means that in the bet-hedging process mentioned earlier (LEVY *et al.* 2012;

GASCH *et al.* 2017), only one in a million cells has serendipitously activated, before desiccation, the ESR defenses needed to survive. In other yeast experiments that uncovered processes or molecules protecting cells from desiccation damage (CALAHAN *et al.* 2011; WELCH *et al.* 2013; TAPIA *et al.* 2015; KIM *et al.* 2018), desiccation tolerance could be experimentally increased up to 10^6 fold relative to normal "unprepared" yeast as increasingly larger fractions of cells expressed their defenses before desiccation was applied. Our intron-bearing mutants are 40 to 1700 times more resistant to desiccation than the wildtype strain, depending on intron position and number (Fig 10). The highest resistance corresponds to only 2.6% of cells surviving desiccation, with bet-hedging still occurring, although resistance is spread to many more cells than in the YJ0 wildtype. Our desiccation results parallel those by WELCH *et al.* (2013), who inhibited ribosomal biogenesis through the TOR pathway in two specific ways, by treating yeast with rapamycin or by deleting the TOR effector SFP1 which is a positive regulator of ribosomal protein and assembly genes. Either method increased desiccation resistance. In addition, they tested 41 temperature sensitive (Ts) ribosome assembly protein mutants which, like our intron mutants, impaired ribosome assembly independently of TOR/PKA. Also like ours, the Ts mutations were expressed in liquid media before desiccation, and all produced various degrees of desiccation resistance, the highest matching the 2-3% resistance of our double mutant. In normal intronless yeast, the highest measured desiccation resistances (up to 40%) are reached during nutrient limitation in stationary phase (CALAHAN *et al.* 2011), but most cells still die. Thus, neither 2 introns per rDNA repeat nor stationary phase growth eliminate bet hedging in yeast. In lichen fungi however, we propose that the new regulatory layers added to the ESR by their many rDNA introns would maintain a semi-constitutive RiBi depression and iESR activation throughout the entire hyphal network even in absence of desiccation, extending protection to the entire thallus (Fig 13). Such readiness might speed further iESR activation at the onset of desiccation.

In contrast to RiBi repression, trehalose induction requires more than one intron

Specific anti-desiccation iESR molecules identified in yeast include the disaccharide trehalose and Hsp12, a small, conformationally flexible heat-shock protein, both of which reduce protein misfolding and aggregation *in vitro* and *in vivo* (KIM *et al.* 2018). As the cytoplasm becomes increasingly dehydrated in presence of high concentrations of trehalose, it transitions into an amorphous solidified state (vitrification). This involves a strong, if disordered, hydrogen bond network through which trehalose and residual water preserve structure and function in biological macromolecules (OLGENBLUM *et al.* 2020).

Trehalose was detected only in the double-intron mutant M-d (Fig. 11) at a concentration of 14 µg/ml. This is too low to account for this strain's 2.6% desiccation tolerance (Fig. 10), as yeast tolerances around 1% require trehalose concentrations between 150 µg/ml (Fig 2 in TAPIA *et al.* (2015)) and 700 µg/ml (Fig 2B in TAPIA AND KOSHLAND (2014)), depending on the experiment. This suggests that most of the desiccation resistance in our yeast mutants is not due to trehalose but to the RiBi repression induced by rDNA introns during environmentally unstressed growth in rich liquid medium. Thus, the RiBi downturns appear to be epistatic (Fig 13) over TOR/PKA, since in the single-intron mutants TOR/PKA remains active and the iESR inactive, as suggested by the absence of trehalose induction (Fig.11). However, the slight activation of trehalose biosynthesis in the double mutant suggests that iESR upregulation begins once the number of introns increases from one to two per repeat, perhaps corresponding to partial feedback downregulation of TOR/PKA (Fig. 13). In lichens therefore, the full operation of the semi-constitutive defense layer may involve multiple introns per repeat, high trehalose concentrations, and perhaps the operation of Hsp12

homologs and other Hsps. We found potential Hsp12 homologs in all lichen fungi whose genomes we queried (Fig. 14). We also queried those genomes for homologs of the yeast TPS1 protein, the first committed trehalose biosynthesis enzyme. Five did encode a protein highly similar to the yeast TPS1 protein (not shown), but such a protein was not retrieved from the *Lobaria pulmonaria* and *Xanthoria parietina* genomes. The occurrence of trehalose in lichens remains to be assessed

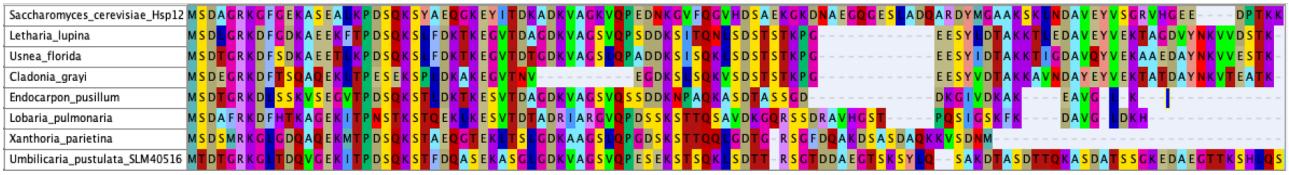

Figure 14. Putative lichen Hsp12 homologs, aligned to *S. cerevisiae* Hsp12. Using as query yeast Hsp12 (https://www.yeastgenome.org/), the sequences shown were retrieved through BLAST (ALTSCHUL *et al.* 1990) from the proteome data of the seven listed lichen fungi. The *L. lupina* and *U. pustlata* genomes were respectively from https://www.ncbi.nlm.nih.gov/bioproject/670757 and https://www.ncbi.nlm.nih.gov/assembly/GCA_900169345.1/; the others from https://genome.jgi.doe.gov/portal/. The alignment was done with ClustalO (SIEVERS *et al.* 2011). The proteins are ~80 to110 AA long, except that from *U. pustulata*, which has an extra 150 aminoacid-long C-terminal region extending beyond the depicted sequence.

directly. Polyols, sugar alcohols protective against osmotic stress and desiccation (HELL *et al.* 2021) are reported to be the predominant soluble carbohydrates in lichens, at 1% to 10% of dry weight, mostly as glycosides (LEWIS AND SMITH 1967). However, even if the involvement of trehalose or other protective solutes in lichen desiccation tolerance remains undetermined, their activity is implicated by the fact that the lichen cytoplasm transitions during desiccation from a highly viscous "rubbery" state around 15% water to an essentially solid vitreous state at 3% water content (CANDOTTO CARNIEL *et al.* 2020), a behavior that resembles vitrification of the drying yeast cytoplasm at high trehalose concentrations (SCHEBOR *et al.* 2000).

In conclusion, we demonstrate that yeast desiccation tolerance is strongly enhanced by the introduction into its rDNA of lichen introns requiring spliceosomes for removal. Based on the yeast responses to intron presence, we hypothesize that the numerous and uniquely altered rDNA introns present in lichens provide protection from extreme desiccation damage by preparing the desiccation stress responses of lichen mycobionts even under unstressed conditions. The evolution of a specific splicing machinery for the degenerate group I introns turned them into repressors of rRNA processing and ribosome assembly, transforming genetic parasites into a new tool to employ against environmental stress; the ectopic rDNA location of spliceosomal introns turned them into repressors of ribosomal protein synthesis to the same purpose. Evolutionarily, the spreading of modified introns into the rDNA of lichen fungi was a watershed moment that allowed lichens to adapt to their permanent exposure to ever-changing environments. The price they paid was slow growth.

Acknowledgments

We thank John Mercer for useful discussions; Vivian Miao, John Woolford, and Austen Ganley for critical reading of the manuscript; Duke University Undergraduate Research Support for funding L.C.; Duke University Trinity College of Arts and Sciences for teaching lab funds for D.A.; 73 individuals, through experiment.com, for research support for D.A. and L.C. The authors declare no competing financial interests.

References

Ahmadjian, V., 1961 Studies on Lichenized Fungi. The Bryologist 64**:** 168-179.

Altschul, S. F., W. Gish, W. Miller, E. W. Myers and D. J. Lipman, 1990 Basic Local Alignment Search Tool. Journal of Molecular Biology 215**:** 403-410.

Ares, M., L. Grate and M. H. Pauling, 1999 A handful of intron-containing genes produces the lion's share of yeast mRNA. RNA 5**:** 1138-1139.

Armaleo, D., and S. May, 2009 Sizing the fungal and algal genomes of the lichen Cladonia grayi through quantitative PCR. Symbiosis 49**:** 43-51.

Armaleo, D., O. Muller, F. Lutzoni, O. S. Andresson, G. Blanc *et al.*, 2019 The lichen symbiosis re-viewed through the genomes of Cladonia grayi and its algal partner Asterochloris glomerata. BMC Genomics 20.

Arnold, A. E., J. Miadlikowska, K. L. Higgins, S. D. Sarvate, P. Gugger *et al.*, 2009 A phylogenetic estimation of trophic transition networks for ascomycetous fungi: are lichens cradles of symbiotrophic fungal diversification? Systematic Biology 58**:** 283-297.

Aschenbrenner, I. A., T. Cernava, G. Berg and M. Grube, 2016 Understanding Microbial Multi-Species Symbioses. Frontiers in Microbiology 7.

Bhattacharya, D., T. Friedl and G. Helms, 2002 Vertical evolution and intragenic spread of lichen-fungal group I introns. Journal of Molecular Evolution 55**:** 74-84.

Bhattacharya, D., F. Lutzoni, V. Reeb, D. Simon, J. Nason *et al.*, 2000 Widespread occurrence of spliceosomal introns in the rDNA genes of ascomycetes. Molecular Biology and Evolution 17**:** 1971-1984.

Birnboim, H. C., and J. Doly, 1979 A rapid alkaline extraction procedure for screening recombinant plasmid DNA. Nucleic Acids Res 7**:** 1513-1523.

Brehm, S. L., and T. R. Cech, 1983 The fate of an intervening sequence RNA: Excision and cyclization of the Tetrahymena ribosomal RNA intervening sequence in vivo. Biochemistry 22**:** 2390-2397.

Calahan, D., M. Dunham, C. DeSevo and D. E. Koshland, 2011 Genetic Analysis of Desiccation Tolerance in Saccharomyces cerevisiae. Genetics 189**:** 507-519.

Candotto Carniel, F., B. Fernandez-Marín, E. Arc, T. Craighero, J. M. Laza *et al.*, 2020 How dry is dry? Molecular mobility in relation to thallus water content in a lichen. Journal of Experimental Botany**:** 1576–1588.

Cech, T. R., 1990 Self-Splicing of Group-I Introns. Annual Review of Biochemistry 59**:** 543-568.

Chiou, L., and D. Armaleo, 2018 A method for simultaneous targeted mutagenesis of all nuclear rDNA repeats in Saccharomyces cerevisiae using CRISPR-Cas9. bioRxiv**:** 276220.

Culberson, C. F., and D. Armaleo, 1992 Induction of a Complete Secondary-Product Pathway in a Cultured Lichen Fungus. Experimental Mycology 16**:** 52-63.

Delarue, M., G. P. Brittingham, S. Pfeffer, I. V. Surovtsev, S. Pinglay *et al.*, 2018 mTORC1 Controls Phase Separation and the Biophysical Properties of the Cytoplasm by Tuning Crowding. Cell 174**:** 338-349.

DePriest, P. T., 1993a Molecular genetic analysis of ribosomal DNA polymorphism in the Cladonia chlorophaea complex, pp. in *Ph.D. Thesis, Duke University* Duke University.

DePriest, P. T., 1993b Small-Subunit rDNA Variation in a Population of Lichen Fungi Due to Optional Group-I Introns. Gene 134**:** 67-74.

DePriest, P. T., and M. D. Been, 1992 Numerous group I introns with variable distributions in the ribosomal DNA of a lichen fungus. Journal of Molecular Biology 228**:** 315-321.

Dez, C., and D. Tollervey, 2004 Ribosome synthesis meets the cell cycle. Curr Opin Microbiol 7**:** 631-637.

Dupuis-Sandoval, F., M. Poirier and M. S. Scott, 2015 The emerging landscape of small nucleolar RNAs in cell biology. Wiley Interdisciplinary Reviews-RNA 6**:** 381-397.

Emri, T., V. Szarvas, E. Orosz, K. Antal, H. Park *et al.*, 2015 Core oxidative stress response in Aspergillus nidulans. BMC Genomics 16.

Gargas, A., P. T. DePriest and J. W. Taylor, 1995 Positions of multiple insertions in SSU rDNA of lichen-forming fungi. Molecular Biology and Evolution 12**:** 208-218.

Gasch, A. P., 2007 Comparative genomics of the environmental stress response in ascomycete fungi. Yeast 24**:** 961-976.

Gasch, A. P., P. T. Spellman, C. M. Kao, O. Carmel-Harel, M. B. Eisen *et al.*, 2000 Genomic Expression Programs in the Response of Yeast Cells to Environmental Changes. Molecular Biology of the Cell 11**:** 4241-4257.

Gasch, A. P., F. B. Yu, J. Hose, L. E. Escalante, M. Place *et al.*, 2017 Single-cell RNA sequencing reveals intrinsic and extrinsic regulatory heterogeneity in yeast responding to stress. Plos Biology 15.

Gasulla, F., E. M. del Campo, L. M. Casano and A. Guéra, 2021 Advances in Understanding of Desiccation Tolerance of Lichens and Lichen-Forming Algae. Plants 10**:** 807.

Gibney, P. A., A. Schieler, J. C. Chen, J. D. Rabinowitz and D. Botstein, 2015 Characterizing the in vivo role of trehalose in Saccharomyces cerevisiae using the AGT1 transporter. Proceedings of the National Academy of Sciences of the United States of America 112**:** 6116-6121.

Hagiwara, D., K. Sakamoto, K. Abe and K. Gomi, 2016 Signaling pathways for stress responses and adaptation in Aspergillus species: stress biology in the post-genomic era. Bioscience Biotechnology and Biochemistry 80**:** 1667-1680.

Haugen, P., V. Reeb, F. Lutzoni and D. Bhattacharya, 2004a The evolution of homing endonuclease genes and group I introns in nuclear rDNA. Molecular Biology and Evolution 21**:** 129-140.

Haugen, P., H. J. Runge and D. Bhattacharya, 2004b Long-term evolution of the S788 fungal nuclear small subunit rRNA group I introns. RNA 10**:** 1084-1096.

Hedberg, A., and S. D. Johansen, 2013 Nuclear group I introns in self-splicing and beyond. Mobile DNA 4.

Hell, A. F., F. Gasulla, M. González-Houcarde, M. T. Pelegrino, A. B. Seabra *et al.*, 2021 Polyols-related gene expression is affected by cyclic desiccation in lichen microalgae. Environmental and Experimental Botany 185**:** 104397.

Hemsley, A., N. Arnheim, M. D. Toney, G. Cortopassi and D. J. Galas, 1989 A Simple Method for Site-Directed Mutagenesis Using the Polymerase Chain-Reaction. Nucleic Acids Research 17**:** 6545-6551.

Ho, Y. H., E. Shishkova, J. Hose, J. J. Coon and A. P. Gasch, 2018 Decoupling Yeast Cell Division and Stress Defense Implicates mRNA Repression in Translational Reallocation during Stress. Current Biology 28**:** 2673-2680.

Hoffman, C. S., and F. Winston, 1987 A ten-minute DNA preparation from yeast efficiently releases autonomous plasmids for transformation of Escherichia coli. Gene 57**:** 267-272.

Honegger, R., 2012 The Symbiotic Phenotype of Lichen-Forming Ascomycetes and Their Endo- and Epibionts in *Fungal Associations. The Mycota (A Comprehensive Treatise on Fungi as Experimental Systems for Basic and Applied Research)* edited by B. Hock. Springer, Berlin, Heidelberg.

Huo, L., R. Wu, Z. Yu, Y. Zhai, X. Yang *et al.*, 2012 The Rix1 (Ipi1p-2p-3p) complex is a critical determinant of DNA replication licensing independent of their roles in ribosome biogenesis. Cell Cycle 11**:** 1325-1339.

Jackson, S. A., S. Koduvayur and S. A. Woodson, 2006 Self-splicing of a group I intron reveals partitioning of native and misfolded RNA populations in yeast. RNA 12**:** 2149-2159.

Junttila, S., A. Laiho, A. Gyenesei and S. Rudd, 2013 Whole transcriptome characterization of the effects of dehydration and rehydration on Cladonia rangiferina, the grey reindeer lichen. BMC Genomics 14.

Kim, S. X., G. Camdere, X. C. Hu, D. Koshland and H. Tapia, 2018 Synergy between the small intrinsically disordered protein Hsp12 and trehalose sustain viability after severe desiccation. Elife 7.

Klinge, S., and J. L. Woolford, 2019 Ribosome assembly coming into focus. Nature Reviews Molecular Cell Biology 20**:** 116-131.

Koshland, D., and H. Tapia, 2019 Desiccation tolerance: an unusual window into stress biology. Molecular Biology of the Cell 30**:** 737-741.

Kranner, I., R. Beckett, A. Hochman and T. H. Nash, 2008 Desiccation-tolerance in lichens: a review. Bryologist 111**:** 576-593.

Kupfer, D. M., S. D. Drabenstot, K. L. Buchanan, H. S. Lai, H. Zhu *et al.*, 2004 Introns and splicing elements of five diverse fungi. Eukaryotic Cell 3**:** 1088-1100.

Lambowitz, A., M. Caprara, S. Zimmerly and P. Perlman, 1999 18 Group I and Group II Ribozymes as RNPs: Clues to the Past and Guides to the Future. Cold Spring Harbor Monograph Archive 37**:** 451-485.

Leprince, O., and J. Buitink, 2015 Introduction to desiccation biology: from old borders to new frontiers. Planta 242**:** 369-378.

Levy, S. F., N. Ziv and M. L. Siegal, 2012 Bet Hedging in Yeast by Heterogeneous, Age-Correlated Expression of a Stress Protectant. Plos Biology 10.

Lewis, D. H., and D. C. Smith, 1967 Sugar Alcohols (Polyols) in Fungi and Green Plants .I. Distribution Physiology and Metabolism. New Phytologist 66**:** 143-184.

Lin, J., and V. M. Vogt, 1998 I-PpoI, the endonuclease encoded by the group I intron PpLSU3, is expressed from an RNA polymerase I transcript. Molecular and Cellular Biology 18**:** 5809-5817.

Liu, R., W. Kim, J. A. Paguirigan, M.-H. Jeong and J.-S. Hur, 2021 Establishment of Agrobacterium tumefaciens-Mediated Transformation of Cladonia macilenta, a Model Lichen-Forming Fungus. Journal of Fungi 7**:** 252.

Morgan, J. T., G. R. Fink and D. P. Bartel, 2019 Excised linear introns regulate growth in yeast. Nature 565**:** 606-611.

Muscarella, D. E., and V. M. Vogt, 1993 A mobile group-I intron from Physarum polycephalum can insert itself and induce point mutations in the nuclear ribosomal DNA of Saccharomyces cerevisiae. Molecular and Cellular Biology 13**:** 1023-1033.

Nielsen, H., and J. Engberg, 1985 Functional intron+ and intron- rDNA in the same macronucleus of the ciliate Tetrahymena pigmentosa. Biochimica Et Biophysica Acta 825**:** 30-38.

Olgenblum, G. I., L. Sapir and D. Harries, 2020 Properties of Aqueous Trehalose Mixtures: Glass Transition and Hydrogen Bonding. Journal of Chemical Theory and Computation 16**:** 1249-1262.

Osheim, Y. N., S. L. French, K. M. Keck, E. A. Champion, K. Spasov *et al.*, 2004 Pre-18S ribosomal RNA is structurally compacted into the SSU processome prior to being cleaved from nascent transcripts in Saccharomyces cerevisiae. Mol Cell 16**:** 943-954.

Parenteau, J., L. Maignon, M. Berthoumieux, M. Catala, V. Gagnon *et al.*, 2019 Introns are mediators of cell response to starvation. Nature 565**:** 612-617.

Pechmann, S., F. Willmund and J. Frydman, 2013 The Ribosome as a Hub for Protein Quality Control. Molecular Cell 49**:** 411-421.

Pfaffl, M. W., 2001 A new mathematical model for relative quantification in real-time RT-PCR. Nucleic Acids Research 29**:** e45.

Poverennaya, I. V., and M. A. Roytberg, 2020 Spliceosomal Introns: Features, Functions, and Evolution. Biochemistry-Moscow 85**:** 725-734.

Protocols, C. S. H., 2006 LB (Luria-Bertani) liquid medium, pp. pdb.rec8141.

Protocols, C. S. H., 2010 Yeast extract-peptone-dextrose growth medium (YEPD), pp. pdb.rec12161.

Reeb, V., P. Haugen, D. Bhattacharya and F. Lutzoni, 2007 Evolution of Pleopsidium (Lichenized ascomycota) S943 group I introns and the phylogeography of an intron-encoded putative homing endonuclease. Journal of Molecular Evolution 64**:** 285-298.

Ryan, O. W., and J. H. D. Cate, 2014 Chapter Twenty-Two - Multiplex Engineering of Industrial Yeast Genomes Using CRISPRm, pp. 473-489 in *Methods in Enzymology*, edited by J. A. Doudna and E. J. Sontheimer. Academic Press.

Ryan, O. W., S. Poddar and J. H. D. Cate, 2016 CRISPR–Cas9 Genome Engineering in Saccharomyces cerevisiae Cells. Cold Spring Harbor Protocols 2016**:** pdb.prot086827.

Saini, K. C., S. Nayaka and F. Bast, 2019 Diversity of Lichen Photobionts: Their Coevolution and Bioprospecting Potential. Microbial Diversity in Ecosystem Sustainability and Biotechnological Applications, Vol 2: Soil & Agroecosystems**:** 307-323.

Salim, D., W. D. Bradford, A. Freeland, G. Cady, J. M. Wang *et al.*, 2017 DNA replication stress restricts ribosomal DNA copy number. Plos Genetics 13.

Sanchez, J. C., A. Ollodart, C. R. L. Large, C. Clough, G. M. Alvino *et al.*, 2019 Phenotypic and Genotypic Consequences of CRISPR/Cas9 Editing of the Replication Origins in the rDNA of Saccharomyces cerevisiae. Genetics 213**:** 229-249.

Sancho, L. G., T. G. A. Green and A. Pintadoa, 2007 Slowest to fastest: Extreme range in lichen growth rates supports their use as an indicator of climate change in Antarctica. Flora 202**:** 667-673.

Schebor, C., M. Galvagno, M. D. Buera and J. Chirife, 2000 Glass transition temperatures and fermentative activity of heat-treated commercial active dry yeasts. Biotechnology Progress 16**:** 163-168.

Sievers, F., A. Wilm, D. Dineen, T. J. Gibson, K. Karplus *et al.*, 2011 Fast, scalable generation of high-quality protein multiple sequence alignments using Clustal Omega. Molecular Systems Biology 7**:** 539.

Stafford, G. A., and R. H. Morse, 1998 Mutations in the AF-2/hormone-binding domain of the chimeric activator GAL4.estrogen receptor.VP16 inhibit hormone-dependent transcriptional activation and chromatin remodeling in yeast. Journal of Biological Chemistry 273**:** 34240-34246.

Tapia, H., and D. E. Koshland, 2014 Trehalose Is a Versatile and Long-Lived Chaperone for Desiccation Tolerance. Current Biology 24**:** 2758-2766.

Tapia, H., L. Young, D. Fox, C. R. Bertozzi and D. Koshland, 2015 Increasing intracellular trehalose is sufficient to confer desiccation tolerance to Saccharomyces cerevisiae. Proceedings of the National Academy of Sciences of the United States of America 112**:** 6122-6127.

Terhorst, A., A. Sandikci, A. Keller, C. A. Whittaker, M. J. Dunham *et al.*, 2020 The environmental stress response causes ribosome loss in aneuploid yeast cells. Proceedings of the National Academy of Sciences of the United States of America 117**:** 17031-17040.

Tripathi, K., N. Matmati, W. J. Zheng, Y. A. Hannun and B. K. Mohanty, 2011 Cellular Morphogenesis Under Stress Is Influenced by the Sphingolipid Pathway Gene ISC1 and DNA Integrity Checkpoint Genes in Saccharomyces cerevisiae. Genetics 189**:** 533-547.

Tuovinen, V., S. Ekman, G. Thor, D. Vanderpool, T. Spribille *et al.*, 2019 Two Basidiomycete Fungi in the Cortex of Wolf Lichens. Current Biology 29**:** 476-483.e475.

Wang, Y., X. Zhang, Q. Zhou, X. Zhang and J. Wei, 2015 Comparative transcriptome analysis of the lichen-forming fungus Endocarpon pusillum elucidates its drought adaptation mechanisms. Science China Life Sciences 58**:** 89-100.

Wang, Y. Y., X. L. Wei, Z. Y. Bian, J. C. Wei and J. R. Xu, 2020 Coregulation of dimorphism and symbiosis by cyclic AMP signaling in the lichenized fungus Umbilicaria muhlenbergii. Proceedings of the National Academy of Sciences of the United States of America 117**:** 23847-23858.

Welch, A. Z., P. A. Gibney, D. Botstein and D. E. Koshland, 2013 TOR and RAS pathways regulate desiccation tolerance in Saccharomyces cerevisiae. Molecular Biology of the Cell 24**:** 115-128.

Welch, A. Z., and D. E. Koshland, 2013 A simple colony-formation assay in liquid medium, termed 'tadpoling', provides a sensitive measure of Saccharomyces cerevisiae culture viability. Yeast 30**:** 501-509.

Zhang, Y., Z. Yu, X. Fu and C. Liang, 2002 Noc3p, a bHLH protein, plays an integral role in the initiation of DNA replication in budding yeast. Cell 109**:** 849-860.